MICHIGAN STATE UNIVERSITY

CYCLOTRON LABORATORY

STUDY OF THE $^{30}Si(^{3}He, p)^{32}P$ REACTION

H. NANN, U. FRIEDLAND, B. HUBERT, W. PATSCHER
and B.H. WILDENTHAL

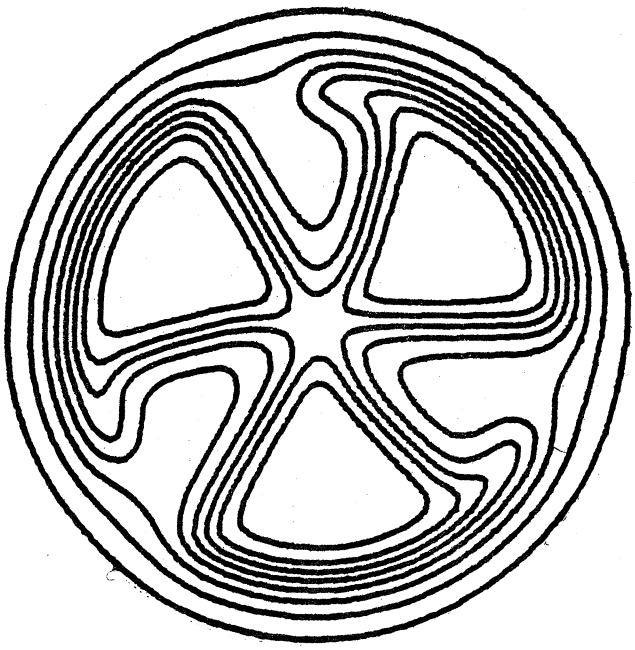

MSUCL-140 AUGUST 1974

Study of the $^{30}Si(^{3}He,p)^{32}P$ Reaction

H. Nann,[+] U. Friedland, B. Hubert[++] and W. Patscher
Institut für Kernphysik der Universität Frankfurt/M, Germany[*]

and

B.H. Wildenthal

Cyclotron Laboratory[**] and Physics Department
Michigan State University, East Lansing, Michigan 48824

ABSTRACT

The $^{30}Si(^{3}He,p)^{32}P$ reaction was studied at an incident energy of 28 MeV, and angular distributions were measured for states in ^{32}P up to 3.00 MeV of excitation energy. Comparison of the experimental differential cross sections with two-nucleon transfer distorted-wave Born approximation (DWBA) calculations was made to test different sets of wave functions, which were calculated in the same configuration space but with different treatments of the effective residual interaction.

E | NUCLEAR REACTION: $^{30}Si(^{3}He,p)^{32}P$, E=28 MeV, measured $\sigma(\theta)$; enriched target; DWBA-analysis.

+ Present address: Cyclotron Laboratory, Michigan State University, East Lansing, Mi. 48824.

++ Present address: Kraftwerk Union, Offenbach, Germany.

* Research supported in part by the Bundesministerium für Forschung und Technologie of the Federal Republic of Germany.

** Research supported in part by the U.S. National Science Foundation.

Introduction

As has been discussed in the literature,[1-6] the comparison of the results of two-nucleon transfer experiments with the predictions obtained from DWBA calculations which employ form-factors derived from detailed nuclear structure calculations constitutes a potentially sensitive test of the theoretical wave functions employed. This report represents part of a systematic investigation of the two nucleon transfer reaction ($^{3}He,p$) on sd-shell nuclei, the aims of which are to delineate the extent to which the two-nucleon transfer data can provide a reliable critique of the structure theory prediction and, to the degree that this appears possible, to test presently available wave functions for states in this region.

In the case of the reaction under study here, $^{30}Si(^{3}He,p)^{32}P$, wave functions for states of both the target and the final nucleus have been calculated in a shell-model study carried out by Wildenthal, et al.[7] These authors employed a truncated $1d_{5/2}$-$2s_{1/2}$-$1d_{3/2}$ basis space, in which the number of particles occupying the $1d_{5/2}$ orbit is limited to be greater than or equal to 10. Two different empirical Hamiltonians were diagonalized in this space. One Hamiltonian was constrained to the form of the modified surface delta interaction (MSDI), and we refer to wave functions obtained with this interaction as MSDI wave functions. The second Hamiltonian was based on the MSDI as a starting point, but the two-body matrix elements which do not

involve the $1d_{5/2}$ orbit were then treated as independent free parameters and adjusted to best fit experimental excitation energies. We refer to wave functions from this interaction as the FPSDI wave functions. In addition to these wave functions we calculated a third set for the ground state of ^{30}Si and the 0^+ and 1^+ (T=1) states of ^{32}P in the same configuration space as above. In this case a realistic effective two-body interaction, deduced from the Sussex relative oscillator matrix elements[8] and corrected for core-polarization and space truncation effects, was used as the Hamiltonian. The single particle energies were taken from the ^{17}O experimental spectrum. In the following we refer to wave functions obtained with this interaction as the SUSSEX wave functions.

In the following we present angular distributions of the $^{30}Si(^3He,p)^{32}P$ reaction for transitions to energy levels in the final nucleus up to 3.0 MeV in excitation. Wherever the final states could be identified with states predicted by the shell-model calculations described above, distorted wave Born approximation (DWBA) calculations based on these wave functions were performed and compared with the data. This comparison suggests possible improvements in the theoretical description of the nuclear states involved.

2. Experimental Procedure and Results

The present study utilized the 28 MeV ^3He beam from the MP tandem accelerator of the Max-Planck-Institut für Kernphysik in Heidelberg. The targets were self-supporting SiO_2 foils,

enriched to 98% in ^{30}Si. The emergent protons were momentum analyzed at 18 angles simultaneously with a multigap magnetic spectrograph and detected in 50 μm Ilford L-4 nuclear emulsions. The emulsions were covered with absorbing foils to stop other impinging charged particles, in particular the deuterons from the $^{30}Si(^3He,d)^{31}P$ reaction. An overall resolution (FWHM) of about 40-45 keV was obtained. A spectrum is shown in fig. 1. Groups corresponding to states in ^{32}P are labelled by their excitation energies; contaminant groups are cross hatched and labelled by the residual nucleus and excitation energy.

The angular distributions for the transitions to levels in ^{32}P up to an excitation energy of 3.0 MeV are displayed in fig. 2. The curves in this figure are results of DWBA calculations and are discussed in detail later. The error bars shown on the experimental data points represent the relative errors. The experimental uncertainty in the absolute cross section is estimated to be approximately 20%.

3. Distorted Wave Analysis

Details of the present method for the DWBA analysis of the $(^3He,p)$ reaction have been described previously.[3] The calculations of the theoretical cross sections have been carried out using the DWBA-code DWUCK.[9] The form factor was calculated separately by the method of Drisko and Rybicki[10] and then fed into DWUCK as data. The optical parameters for calculating the distorted waves in the entrance and exit channels were adapted from the

literature[11,12] and are given in table 1. In order to make the sum over the transferred angular momentum L and spin S in the transition amplitude incoherent, spin-orbit dependent distortions were neglected. No radial cut-offs were used in the present calculations. The spectroscopic amplitudes derived from the above described sets of wave functions for the various transitions analyzed are present in table 2.

The calculated differential cross sections for the transitions to the states in ^{32}P up to an excitation energy of 3.0 MeV are compared in fig. 2 with the experimental data. The full lines represent DWBA calculations based on the FPSDI wave functions. The dashed lines are those based on the MSDI wave functions, and the dashed - dotted lines are those based on the SUSSEX wave functions. Only full lines are shown where the different calculations do not predict significantly different shapes for an angular distribution. Each calculated angular distribution is independently normalized for a best fit to the experimental data. With the assumption of a common normalization, corresponding to $D_o^2 = 20 \times 10^4$ MeV^{2}fm^3, one obtains the ratios σ_{exp}/σ_{th} which are given in table 3. Values in brackets indicate that in these cases the shapes of the angular distributions are not even approximately reproduced by the calculations.

4. Discussion

In the following discussion we restrict ourself to transitions to states in ^{32}P below 3.00 MeV of excitation energy. Angular

distributions to higher excited states were omitted, since these states have either negative parity or their spins and parities are not unambiguously known. In the first case a comparison with nuclear structure calculations cannot be carried out, because no wave functions are available, and in the second case an identification of the calculated and measured levels is not possible. Moreover, even if the spins and parities are known, the wave functions for higher excited states cannot be unambiguously correlated with the experimentally observed states.

4.1 Transition to the 0^+ state at 0.51 MeV.

The experimentally observed strength of this transition is about one order of magnitude smaller than of the other transitions, which indicates a cancellation of different transfer contributions. The three different sets of shell-model wave functions predict a destructive interference between the $(2s_{1/2})^2$ and $(1d_{3/2})^2$ transfer amplitudes with only a small $(1d_{5/2})^2$ admixture (see table 2).

Both the FPSDI and the MSDI wave functions predict an almost completely cancelling $(2s_{1/2})^2$ and $(1d_{3/2})^2$ transfer mixture. Hence, the magnitude of the cross section is underestimated by a factor of more than 100 (see table 3) by both sets and even the shape of the angular distribution is not reproduced correctly. This can happen even for a pure L transfer, where, as it was pointed out in a previous paper,[13] different transfer amplitudes almost completely cancel by destructive interference. An enhancement of the $(2s_{1/2})^2$ spectroscopic

amplitude and a simultaneous reduction of the $(1d_{3/2})^2$ spectroscopic amplitude would effectively produce the right magnitude of the theoretical cross section and would also correctly reproduce the shape. This suggests that the FPSDI and MSDI wave functions of the ground state of ^{30}Si should contain a larger $(1d_{5/2})^{12}\ (1d_{3/2})^2_{0,1}$ and a smaller $(1d_{5/2})^{12}\ (2s_{1/2})^2_{0,1}$ component than occurs in the present calculations. Such a readjustment would also tend to produce better agreement between the experimental and calculated spectroscopic factors for the neutron pick-up leading to the lowest $1/2^+$ and $3/2^+$ states in ^{29}Si (see ref. 14).

The SUSSEX wave functions predict a much larger $(2s_{1/2})^2$ transfer amplitude for this transition than do the FPSDI and MSDI wave functions and give a good account of the shape of the angular distribution (dashed-dotted line in fig. 2). However, they produce a differential cross section which is too large by a factor of two. Here also, a readjustment of the $(1d_{5/2})^{12}\ (1d_{3/2})^2_{0,1}$ and $(1d_{5/2})^{12}\ (2s_{1/2})^2_{0,1}$ components in the ground state wave function of ^{30}Si (but this time in opposite direction as for the FPSDI and MSDI wave functions) would improve the agreement between the calculated magnitude of the cross sections and the experimental data.

4.2 Transitions to the 1^+ states at 0.00, 1.15, 2.23 and 2.74 MeV.

The two-nucleon transfer selection rules allow for the transitions to these 1^+ states a mixture of L=0 and L=2, where

the L=0 contribution is kinematically enhanced over the L=2 admixture.[4] The experimental angular distributions of the transitions to the 0.00 and 2.74 MeV states exhibit predominantly L=2 patterns (see fig. 2), whereas only the transition to the 1.15 MeV state shows the marked structure of a nearly pure L=0 transition. The transition to the 2.23 MeV state could not be experimentally resolved from the transition to the 2.22 MeV state. The experimental angular distribution for this doublet shows an L=2 pattern. The most probable spin assignment[15] to the 2.22 MeV state, 2^+, requires a pure L=2 transition to this state. Hence, the transition to the 1^+ state at 2.23 MeV is unlikely to have a significant L=0 strength.

All three sets of wave functions correctly reproduce the shapes of the angular distributions to the 0.00 and 1.15 MeV states. The FPSDI and MSDI wave functions give a good account of the magnitude of the differential cross section for the ground state transition but not for the 1.15 MeV transition, which is underpredicted by more than a factor of two. The SUSSEX wave functions fail to predict the magnitude for both transitions.

The MSDI and SUSSEX wave functions yield the correct shape of the 2.74 MeV angular distribution but they overestimate the magnitude of the differential cross section by a factor of more than three. The FPSDI wave functions fail to predict correctly either the angular dependence or the magnitude of the differential cross section for this transition.

For the transition to the 2.23 MeV state, only the SUSSEX wave functions predict the nearly pure L=2 angular distribution (dashed-dotted line in fig. 2) which agrees with the experimental data. Both the FPSDI and MSDI wave functions produce a mixture of L=0 and L=2, (the L=0 contribution predicted by the MSDI wave functions is larger than that by the FPSDI wave functions), and hence cannot represent the envelope of the experimental angular distribution.

4.3 Transitions to the 2^+ states at 0.08, 1.32 and 2.66 MeV.

Two-nucleon transfer selection rules restrict these transitions to be pure L=2. In these cases the quantitative nuclear structure information available from the data is contained only in the magnitude of the cross section, since the shape is essentially independent of the details of the nuclear wave functions. Both the FPSDI and MSDI wave functions fail to predict the transition strengths for these transitions to within a factor of two.

4.4 Transitions to the 3^+ states at 1.75, 2.18 and 3.00 MeV.

These states can be populated by a mixture of L=2 and L=4 transfer, which is, indeed, observed experimentally for all three transitions. Both the FPSDI and MSDI wave functions predict mainly $(1d_{3/2})^2_{3,0}$ transfer and give a good account of the shape of the angular distributions.

The strength of the 1.75 MeV transition is well predicted by the FPSDI wave functions, whereas they fail to reproduce the magnitude of the 2.18 and 3.00 MeV cross section by factors

greater than two. The MSDI wave functions predict the strength of the 1.75 and 3.00 MeV transitions correct to within a factor of two.

5. Conclusions

For this paper we have attempted to reproduce the experimental differential cross sections of the $^{30}Si(^3He,p)^{32}P$ reaction with microscopic DWBA calculations based on three sets of shell-model wave functions. These wave functions were obtained from calculations which used identical model basis spaces but different effective Hamiltonians. For most transitions, the three sets of shell-model wave functions failed to predict the magnitudes of the differential cross sections to better than a factor of two. Another difficulty occurred in reproducing the shapes of the experimental angular distributions for transitions to the higher lying 1^+ states in ^{32}P. This is not unexpected because the description of 1^+ states in odd-odd nuclei have always presented considerable problems to shell-model theorists. The relatively successfull representation of the first two 1^+ states is the most significant success of the present wave functions.

From the analysis of the transition to the 0.51 MeV state in ^{32}P it appears that none of the three sets of wave functions studied contain a proper mixture of the main components, $(1d_{5/2})^{12}\ (2s_{1/2})^2_{0,1}$ and $(1d_{5/2})^{12}\ (1d_{3/2})^2_{0,1}$, of the ^{30}Si ground state wave function. A readjustment of the strength of these two components can produce better agreement between the experimental data and the calculated cross sections. The adjustments

suggested, for the FPSDI and MSDI wave functions an increase of the $(1d_{3/2})^2_{0,1}$ component and a reduction of the $(2s_{1/2})^2_{0,1}$ component, also account for a better agreement between the experimental and calculated spectroscopic factors for one-nucleon pick-up reactions on ^{30}Si.

The present two-nucleon transfer results show that the investigated shell-model calculations fail to account for the wave functions of the ground state of ^{30}Si and the low lying states of ^{32}P with consistent quantitative accuracy. This conclusion is supported by the results of one-nucleon transfer reactions such as $^{30}Si(d,t)^{29}Si$ (ref. 16) and $^{31}P(d,p)^{32}P$ (ref. 17). In both cases the comparison between theoretical and experimental spectroscopic factors show only qualitative agreement with discrepancies of up to 70%. A partial explanation of the failure of the tested FPSDI and MSDI wave functions could be that the occupation of the $1d_{3/2}$ shell is in general underestimated. In order to answer the question of whether this is attributed to the truncated model space or to the effective Hamiltonians used, further shell-model calculations with more realistic matrix elements of the residual interaction in the full 2s-1d basis space should be done.

The authors are indebted to Professors P. Brix, W. Gentner and U. Schmidt-Rohr for the hospitality at the Max-Planck-Institut für Kernphysik in Heidelberg. It is also a pleasure to thank Drs. H.H. Duhm and H. Hafner for their help during the experiments and for the assistance in taking the data.

Table 1

Optical-model parameters used in the DWBA calculations.

	V (MeV)	W_v (MeV)	W_s (MeV)	r_o (fm)	a (fm)	r_c (fm)	r_I (fm)	a_I (fm)
^{3}He	173.9	20.6		1.15	0.65	1.40	1.50	0.98
p	45.5		11.5	1.20	0.70	1.25	1.25	0.70

The ^{3}He-parameters are adapted from ref. 11, the p-parameters from ref. 12.

Table 2.

Spectroscopic amplitudes for the $^{30}Si(^3He,p)^{32}P$ reaction.

J_f^π	E_x (MeV)	(J,T)		(D5,D5)	(S1,S1)	(D3,D3)	(D5,S1)	(D5,D3)	(S1,D3)
0^+	0.51	(0,1)	a)	-0.052	+0.279	-0.757			
			b)	+0.044	-0.292	+0.780			
			c)	+0.033	-0.475	+0.514			
1^+	0.00	(1,0)	a)	-0.042	-0.014	+0.250		+0.035	-0.357
			b)	+0.062	+0.042	-0.194		-0.046	+0.425
			c)	-0.016	+0.060	+0.211		+0.005	-0.165
	1.15	(1,0)	a)	+0.028	+0.265	+0.329		-0.029	+0.101
			b)	+0.029	+0.256	-0.089		-0.001	+0.097
			c)	+0.056	+0.496	+0.209		+0.022	+0.036
	2.23	(1,0)	a)	+0.032	+0.202	-0.501		-0.008	-0.218
			b)	+0.010	+0.102	-0.237		-0.010	-0.279
			c)	+0.001	-0.057	-0.392		+0.056	-0.321
	2.74	(1,0)	a)	-0.027	-0.037	+0.258		-0.002	-0.405
			b)	+0.005	-0.157	-0.117		+0.150	-0.010
			c)	-0.024	+0.157	+0.222		-0.026	-0.498
2^+	0.08	(2,0)	a)				+0.055	-0.045	+0.448
			b)				+0.057	-0.043	+0.494
		(2,1)	a)	-0.057		-0.106	-0.085	+0.034	-0.761
			b)	-0.055		-0.166	-0.078	+0.026	-0.755

Table 2. Cont'd.

J_f^π	E_x (MeV)	(J,T)		(D5,D5)	(S1,S1)	(D3,D3)	(D5,S1)	(D5,D3)	(S1,D3)
	1.32	(2,0)	a)				-0.041	-0.054	-0.136
			b)				+0.020	+0.046	+0.084
		(2,1)	a)	+0.015		+0.687	+0.096	+0.051	-0.004
			b)	-0.011		-0.722	-0.065	-0.030	+0.059
	2.22	(2,0)	a)				-0.038	-0.058	+0.193
			b)				+0.069	-0.023	-0.174
		(2,1)	a)	+0.006		-0.126	+0.047	+0.020	+0.229
			b)	-0.007		-0.198	+0.047	-0.006	-0.124
	2.66	(2,0)	a)				-0.012	-0.043	-0.285
			b)				-0.033	+0.036	-0.036
		(2,1)	a)	-0.007		-0.481	+0.090	+0.047	+0.018
			b)	+0.007		+0.217	-0.113	+0.099	-0.113
3^+	1.75	(3,0)	a)	-0.007		+0.617	+0.010	-0.060	
			b)	+0.007		-0.430	-0.057	+0.070	
	2.18	(3,0)	a)	-0.005		+0.363	-0.083	+0.100	
			b)	-0.008		+0.466	-0.102	+0.029	
	3.00	(3,0)	a)	-0.006		+0.195	+0.074	+0.084	
			b)	+0.009		-0.388	-0.041	-0.084	

a) MSDI wave functions.

b) FPSDI wave functions

c) SUSSEX wave functions.

Table 3.

Comparison of experimental and theoretical transition strengths.

$E_x(^{32}P)$ (MeV)	J^π	σ_{exp}/σ_{th} FPSDI	MSDI	SUSSEX
0.00	1^+	0.98	0.05	3.90
0.08	2^+	0.40	0.43	
0.51	0^+	145.0	118.0	0.54
1.15	1^+	2.40	2.30	0.48
1.32	2^+	0.48	0.25	
1.75	3^+	1.02	0.55	
2.18	3^+	0.25	0.40	
2.22	2^+	(0.53)	(0.35)	
2.23	1^+			
2.66	2^+	2.40	0.34	
2.74	1^+	(1.30)	0.30	0.23
3.00	3^+	0.42	1.50	

FIGURE CAPTIONS

Figure 1 Proton spectrum from the $^{30}Si(^{3}He,p)^{32}P$ reaction at 28 MeV bombarding energy and $\theta_{lab} = 20.5°$.

Figure 2 Angular distributions of the $^{30}Si(^{3}He,p)^{32}P$ reactions. The curves correspond to DWBA calculations.

REFERENCES

1. I.S. Towner and J.C. Hardy, Adv. in Phys. 18 (1969)401.
2. W.G. Davies, J.C. Hardy and W. Darcey, Nucl. Phys. A128 (1969)465.
3. H. Nann, B. Hubert and R. Bass, Nucl. Phys. A176 (1971)553.
4. B. Hubert, H. Nann, W. Schäfer and R. Bass, Nucl. Phys. A181 (1972)1.
5. H. Nann, T. Mozgovoy, R. Bass and B.H. Wildenthal, Nucl. Phys. A192 (1972)417.
6. H. Nann, L. Armbruster and B.H. Wildenthal, Nucl. Phys. A198 (1972)11.
7. B.H. Wildenthal, J.B. McGrory, E.C. Halbert and H.D. Graber, Phys. Rev. C4 (1971)1708.
8. S. Maripuu, private communication.
9. P.D. Kunz, University of Colorado, private communication.
10. R.M. Drisko and F. Rybicky, Phys. Rev. Lett. 16 (1966)275.
11. H.P. Morsch and R. Santo, Nucl. Phys. A179 (1972)401.
12. G.W. Greenlees and G.J. Pyle, Phys. Rev. 149 (1966)8361
13. R. Bass, U. Friedland, B. Hubert, H.Nann and A. Reiter, Nucl. Phys. A198 (1972)449.
14. B.H. Wildenthal and J.B. McGrory, Phys. Rev. C7 (1973)714.
15. F.E.H. van Eijkern, G. van Middelkoop, J. Timmer and J.A. van Luijk, Nucl. Phys. A210 (1973)38.
16. D. Dehnhard and J.L. Yntema, Phys. Rev. 163 (1967)1198.
17. J.J.M. van Gasteren, A.J.L. Verhage and J.F. van der Veen, Nucl. Phys. A210 (1973)29.

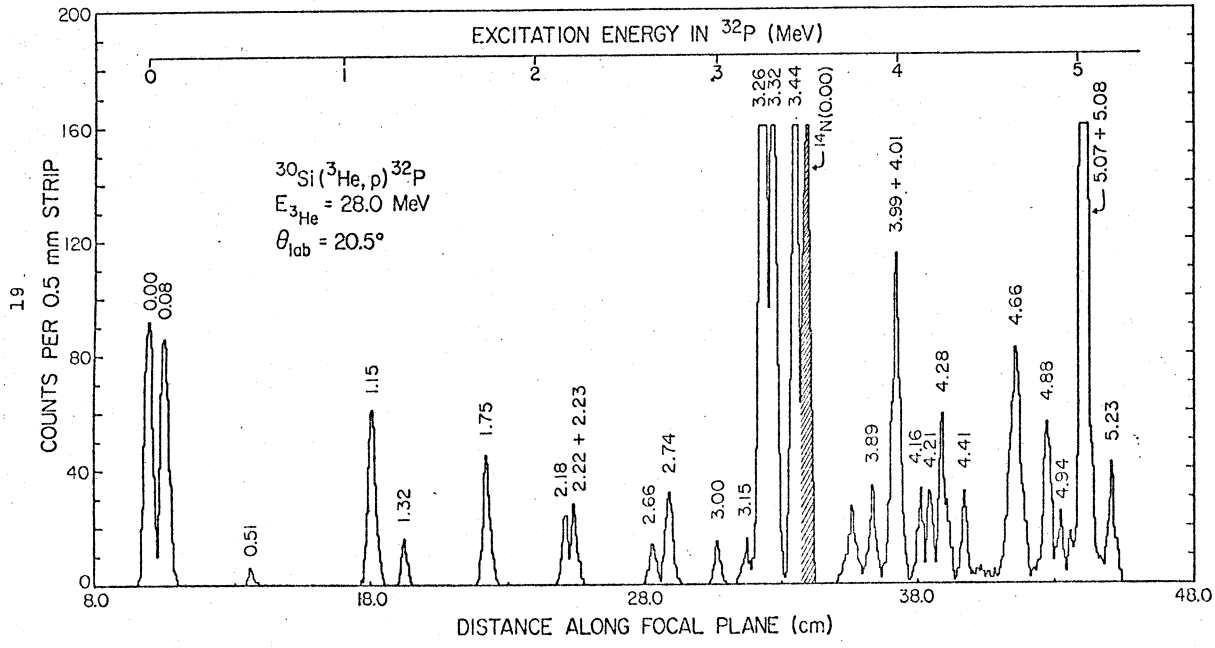
EXCITATION ENERGY IN ^{32}P (MeV)
^{30}Si(^{3}He, p)^{32}P
$E_{^{3}He}$ = 28.0 MeV
θ_{lab} = 20.5°
COUNTS PER 0.5 mm STRIP
DISTANCE ALONG FOCAL PLANE (cm)
0.00
0.08
0.51
1.15
1.32
1.75
2.18
2.22 + 2.23
2.66
2.74
3.00
3.15
3.26
3.32
3.44
^{14}N(0.00)
3.89
3.99 + 4.01
4.16
4.21
4.28
4.41
4.66
4.88
4.94
5.07 + 5.08
5.23

Fig. 1

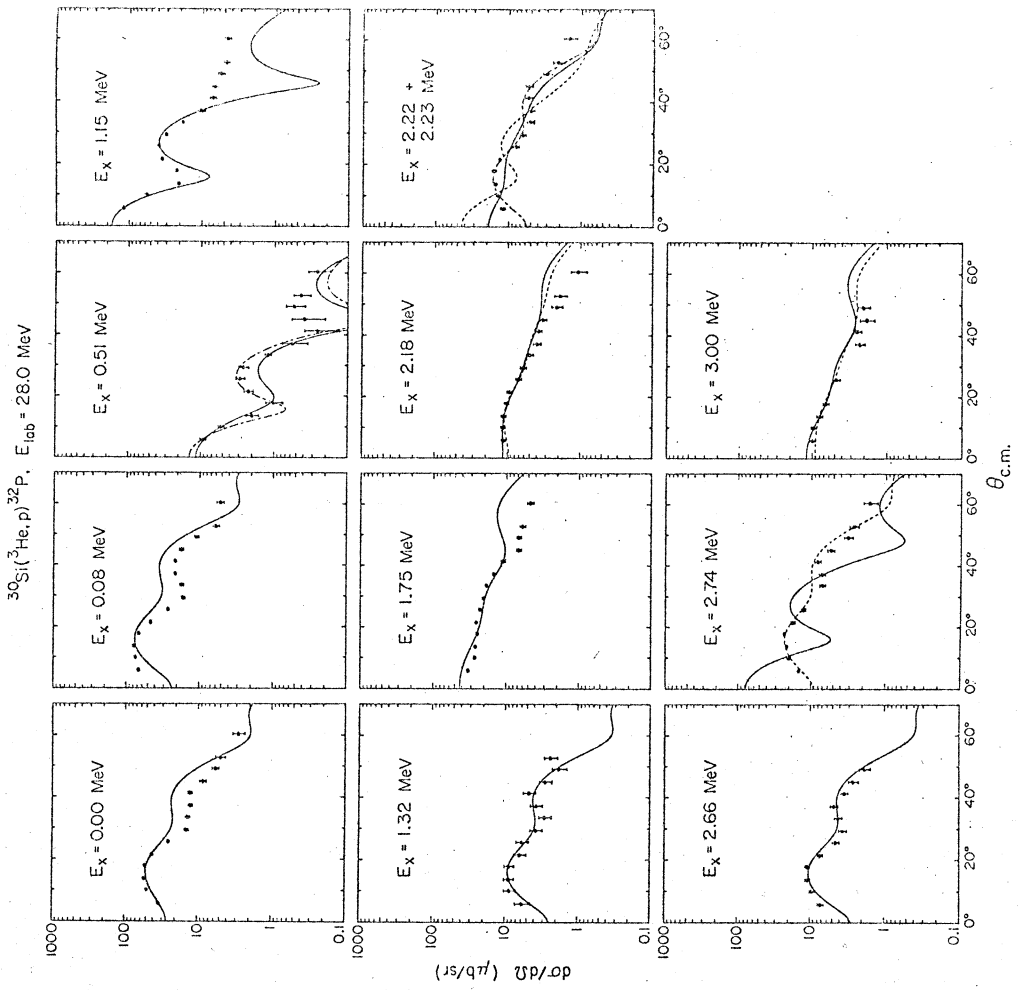
^{30}Si(^{3}He, p)^{32}P, E_{lab} = 28.0 MeV
E_x = 0.00 MeV
E_x = 0.08 MeV
E_x = 0.51 MeV
E_x = 1.15 MeV
E_x = 1.32 MeV
E_x = 1.75 MeV
E_x = 2.18 MeV
E_x = 2.22 + 2.23 MeV
E_x = 2.66 MeV
E_x = 2.74 MeV
E_x = 3.00 MeV
$\theta_{c.m.}$
$d\sigma/d\Omega$ (μb/sr)

Fig. 2